Advances in Radiation Oncology (2016) 1, 194-203

advances in radiation oncology

www.advancesradonc.org

Scientific Article

Feasibility of 4D perfusion CT imaging for the assessment of liver treatment response following SBRT and sorafenib

Catherine Coolens PhD [a,b,c,d,*], Brandon Driscoll MASc [a], Joanne Moseley PhD [a], Kristy K. Brock PhD [e], Laura A. Dawson MD FRCPC [a,b]

[a] *Radiation Medicine Program, Princess Margaret Cancer Center and University Health Network, Toronto, Ontario, Canada*
[b] *Department of Radiation Oncology, University of Toronto, Toronto, Ontario, Canada*
[c] *Institute of Biomaterials and Biomedical Engineering, University of Toronto, Ontario, Canada*
[d] *TECHNA Institute, University Health Network, Toronto, Ontario, Canada*
[e] *Department of Radiation Oncology, University of Michigan, Ann Arbor, Michigan*

Received 28 February 2016; received in revised form 26 April 2016; accepted 22 June 2016

Abstract

Objectives: To evaluate the feasibility of 4-dimensional perfusion computed tomography (CT) as an imaging biomarker for patients with hepatocellular carcinoma and metastatic liver disease.

Methods and materials: Patients underwent volumetric dynamic contrast-enhanced CT on a 320-slice scanner before and during stereotactic body radiation therapy and sorafenib, and at 1 and 3 months after treatment. Quiet free breathing was used in the CT acquisition and multiple techniques (rigid or deformable registration as well as outlier removal) were applied to account for residual liver motion. Kinetic modeling was performed on a voxel-by-voxel basis in the gross tumor volume and normal liver resulting in 3-dimensional parameter maps of blood perfusion, capillary permeability, blood volume, and mean transit time. Perfusion characteristics in the tumor and adjacent liver were correlated with radiation dose distributions to evaluate dose-response. Paired *t* tests assessed change in spatial and histogram parameters from baseline to different time points during and after treatment. Technique reproducibility as well as the impact of arterial and portal vein input functions was also investigated using intra- and inter-subject variance and Bland-Altman analysis.

Results: Quantitative perfusion parameters were reproducible (±5.7%; range, 2%-10%) depending on tumor/normal liver type and kinetic parameter. Statistically significant reductions in tumor perfusion were measurable over the course of treatment and as early as 1 week after sorafenib administration ($P < .05$). Marked liver parenchyma perfusion reduction was seen with a strong dose-response effect ($R^2 = 0.95$) that increased significantly over the course treatment.

Sources of support: This work was supported by the Canadian Institutes of Health Research (grant 202477), Bayer, University of Toronto Dean's Fund (C.C.), Ontario Institute of Cancer Research (grant P.IT.020), and the National Science and Research Council of Canada (grant 354701).

* Corresponding author. Princess Margaret Cancer Centre, Radiation Medicine Program, 610 University Avenue, Toronto ON, M5G 2M9, Canada
E-mail address: catherine.coolens@rmp.uhn.on.ca (C. Coolens)

http://dx.doi.org/10.1016/j.adro.2016.06.004

Conclusions: The proposed methodology demonstrated feasibility of evaluating spatiotemporal changes in liver tumor perfusion and normal liver function following antiangiogenic therapy and radiation treatment warranting further evaluation of biomarker prognostication.

Introduction

Quantitative functional imaging methods have become more prominent in the management of solid tumors for staging of disease, target definition, and early response detection of treatment efficacy.[1,2] Moreover, measuring vascular change is important when optimizing the timing of antiangiogenic therapies and radiation therapy.[3] Dynamic contrast-enhanced (DCE) computed tomography (CT) of the liver, with high resolution and clinical convenience, is a key potential method in this regard.[2] Advances in perfusion imaging analysis techniques and scanner acquisition capabilities have brought voxel-based perfusion imaging of the liver into the realm of possibilities and it is now well-understood that the absence of 3-dimensional (3D) volumetric representation results in poor accuracy and robustness as well as a lack of heterogeneity information, which is much-needed to address and understand changes in tumor behavior and treatment response.[4-6]

Traditionally, motion artifacts resulting from patient movement during image acquisition have further confounded parametric perfusion maps because DCE-CT acquisitions can potentially run up to 4 minutes to do permeability studies.[7] This can create significant problems for CT perfusion, particularly for those organs subject to respiratory motion, such as the lung or liver. Careful instruction to the patient helps to minimize this,[7] but also reduces scan frequency and requires substantial patient cooperation to ensure reproducibility which is not always possible. Respiratory-induced organ movement is largest in the superior-inferior direction[8,9]; therefore, making it almost impossible to compensate for with limited-slice imaging.

Multislice CT technology now provides the possibility of performing fast acquisitions of wide volumetric scans using 256- or 320-slice detectors.[10] This technology offers great advantages over conventional CT perfusion imaging studies and brings the field-of-view (FOV) to levels similar to DCE-magnetic resonance imaging (MRI) scans allowing for true dynamic volume acquisitions without the need to move the couch or detector such that every volume represents a particular respiration phase and intrascan image registration becomes an option. The main goal of the work presented here was to: (1) assess the feasibility of using volumetric CT perfusion to provide 3D perfusion parameter maps in a challenging group of patients with hepatocellular carcinoma (HCC) and liver metastases subject to breathing motion and (2) assess its sensitivity and robustness in capturing changes in liver and tumor perfusion as a response to treatment for use as a noninvasive imaging biomarker. Having the ability to measure permeability and perfusion would be beneficial, especially in this patient group, because these physiological changes can happen long before there is any evidence of tumor volume change seen on conventional imaging and could aid in the early selection of the most appropriate treatment regime.

Methods and materials

Patients and treatment

Patients with liver cancer, being treated as part of a research ethics board (REB)-approved study of liver stereotactic body radiation therapy (SBRT) and sorafenib,[11] underwent volumetric DCE-CT under a further elective REB-approved companion imaging study. Three patients had HCC and 1 had multiple liver metastases, resulting in a total of 6 tumors considered in this study. One tumor had a necrotic core. All patients were surgically unresectable and treated with SBRT and sorafenib with sorafenib doses ranging from 200 to 400 mg by mouth twice daily and SBRT doses ranging between 30 and 54 Gy given in 6 fractions over 2 weeks, on a phase 1 study.[11]

Volumetric liver DCE-CT on a 320-slice CT

Patients had volumetric CT perfusion scans within 2 weeks before RT or sorafenib (baseline), 1 week after the start of sorafenib (pre-RT), in the middle of RT, and 1 and 3 months after treatment. Each scan was acquired under quiet free breathing as a dynamic volume time sequence on a 320-slice CT scanner (Toshiba, Aquilion One)[12] after intravenous injection of iodixanol (Visipaque^{320}, GE Healthcare) at 2 mL/kg (to a maximum of 150 mL) at 4 mL/second with the aim of assessing tumor permeability as well as perfusion. The scan parameters (100 mAs, 120 kV, 0.5-second gantry rotation) were optimized to balance image quality with CT dose and tube heating, resulting in

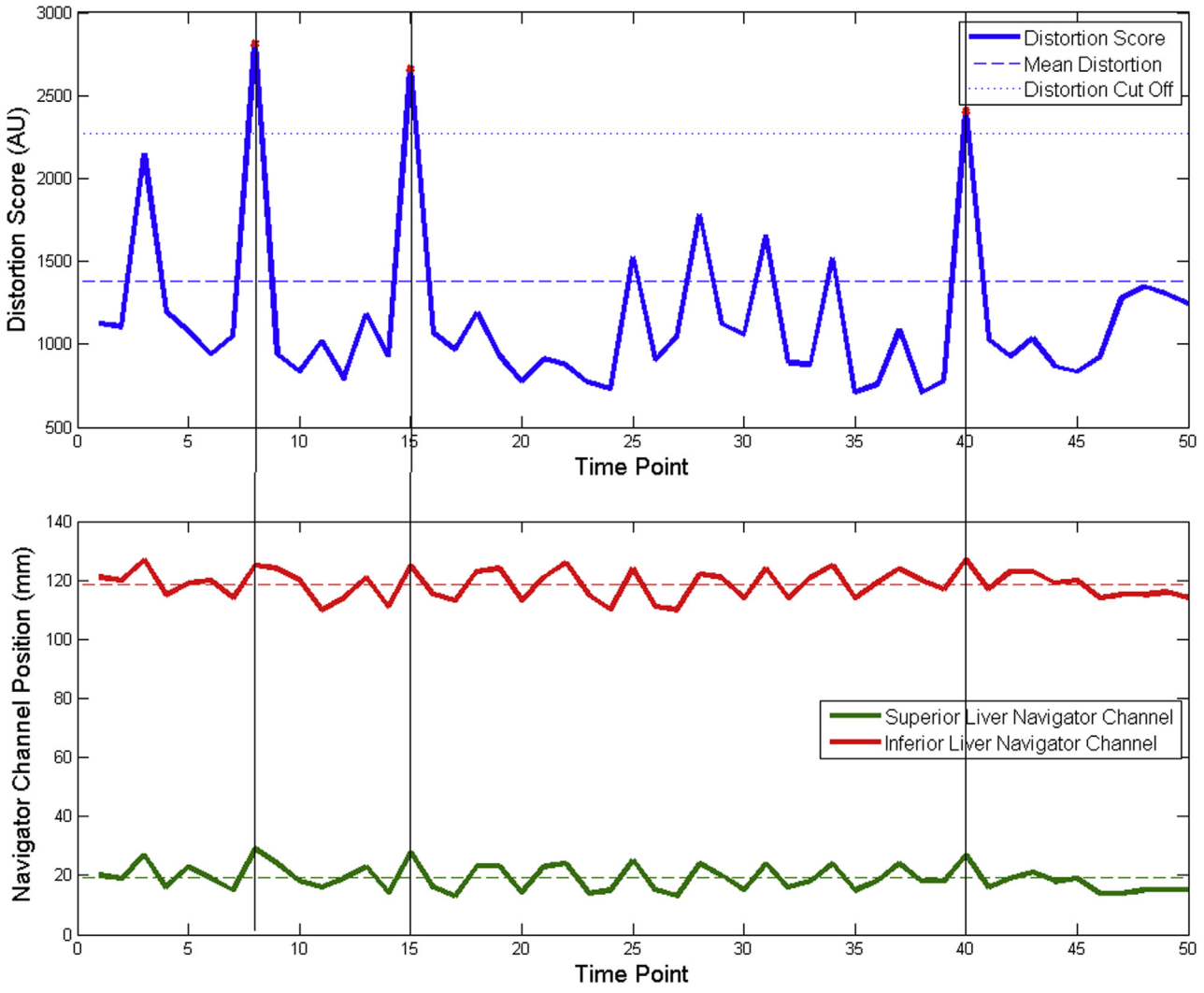

Figure 1 A graphical depiction of the outlier removal method. (Top) The "distortion score" of each volume of the DCE-CT scan is calculated and the points above 1.3 standard deviations from the mean are marked for removal. (Bottom) The dropped points correlate with peaks in the breathing trace. AU, arbitrary unit; K_{trans}, kinetic parameters of perfusion.

the following time sequence: immediately after injection volumes were acquired every 1.5 seconds (until 57 seconds) for fast sampling of the uptake curve and peak enhancement; then at 2.5-second intervals between 65 and 96 seconds; and consequently every 10 seconds until 255 seconds to sample slower changing contrast decrease and allow for permeability modeling. Nominal scan times for assessment of liver vascularity only typically run between 60 and 120 seconds.[13] The resulting volumetric CT dose index ($CTDI_{vol}$) was 60 cGy. This resulted in 60 volumes of 160 slices reconstructed at (0.46 × 0.46 × 1mm) voxel size and 512 × 512 × 320 FOV matrix, allowing coverage of almost the entire liver (or near entire) at each time point (baseline range, 978-1682 mL).

The arterial perfusion and portal venous perfusion CT volumes from the dynamic time sequence were chosen at 20 and 60 seconds, respectively, after the CT signal in the aorta enhanced by 100 Hounsfield units. Arterial perfusion, portal venous perfusion, and parenchyma perfusion volume scans were registered to the arterial perfusion scan from the original planning triphasic data with the intention of correlating perfusion changes with the dose distributions, and assessing whether the perfusion scan could replace the triphasic planning scan for future routine practice. This would further minimize the overall CT scan dose for the patient.

Motion correction and image registration

A finite-element biomechanical motion model was implemented to allow for deformable image registration between all volumes of the volumetric DCE-CT time series.[14] This model was then adapted for each volume using navigator channels, which are rectangular boxes to capture edge detection. These were placed on the dome of

the liver to detect the mean superoinferior displacement shift of the liver in each volume that consequently determined the adaptation level of the motion model to each volume.

However, except for patient 1, even the large 16-cm scan coverage was not always sufficient to have the entire liver visible in every single phase of the DCE-CT time sequence under free breathing conditions to allow the creation of a motion model. Therefore, the use of an automated distortion factor was implemented to quickly evaluate the level of motion distortion by first classifying each voxel of the scan into air, tissue, or bone based on their average precontrast CT number. For each DCE volume, the number of voxels that changed classification from 1 time point to the next was totaled and defined a distortion score (arbitrary unit). Voxels classified as tissue that changed to bone were not counted as they could represent contrast voxels. Volumes, which had a score higher than 1.3 × the standard deviations from the mean score were dropped from the functional analysis data set. This is method is being referred to as the "outlier" approach and the cutoff threshold of 1.3 sigma was determined experimentally based on balancing reducing the extent of motion, as represented by the distortion score, with DCE temporal sampling requirements. As can be seen in Fig 1, the distortion score is synchronized with the navigator channel motion patterns. A comparison between the outlier method, a 1-dimensional rigid registration along the superoinferior direction and a full deformable registration correction was performed on the baseline scan for patient 1 where the breathing extents were available to generate a motion model for the patient. The resulting pharmacokinetic parameter histograms were compared between the 2 techniques.

4D kinetic modeling for volumetric perfusion CT analysis

Kinetic analysis was done on every voxel of the liver, tumor included, using an in-house 4-dimensional (4D) temporal dynamic analysis method, which enables automated parametric analysis based on patient-specific dynamic behavior of contrast flow.[15] This has been validated using a dynamic flow phantom capable of creating typical liver enhancement curves[5,16] and shown to improve sensitivity of perfusion CT as an imaging biomarker in a recent study of brain metastases treated with stereotactic radiosurgery.[4] The modified Tofts model[17] was used to estimate kinetic parameters of perfusion (K_{trans} [mL/g/min]), extracellular volume (v_e [mL/g]), and the whole blood volume per unit of tissue (V_b [mL/g]) because most tumors were HCC[18] and rely on arterial single input flow. Semiquantitative measures of perfusion such as the maximum slope of the uptake curve, maximum contrast intensity, the time-to-maximum intensity, the mean transit time, and the area under the curve (AUC) were also evaluated. The arterial input function (AIF) was chosen in the aorta at the level of the diaphragm because it was the most reproducible and stable measurement of flow.

Reproducibility of perfusion parameters

A repeat baseline DCE-CT scan was conducted in 1 patient (patient 4) 1 day later, to assess perfusion parameter reproducibility. Gross tumor volume (GTV) kinetic parameters as well as unirradiated liver and spleen parenchyma regions of interest (ROIs) were compared on both baseline scans. Bland-Altman analysis was used to determine the reproducibility for direct voxel-to-voxel comparison as well as pooled variation and correlation between the median and skew parameters of the 3D histograms. Although not recommended for routine use, this double baseline was REB-approved for establishing feasibility.

Tumor perfusion changes over time

Voxel-based perfusion parameters were obtained within every GTV and moment analysis was done on the histograms of both AUC and K_{trans} results (ie, calculating the mean, median, standard deviation, skewness, and kurtosis of the distribution in the ROI, with the latter 2 describing the heterogeneity within the tumor). A linear regression was done of the moment analysis results over the course of treatment.

Quantification of liver parenchyma perfusion following treatment

The liver minus GTV was defined as liver parenchyma and the first exhale volume of the DCE-CT scan before contrast arriving was registered to the planning CT scan using ROI-based mutual information. This volume was found by retrospectively observing the liver motion in a reconstructed time sequence and selecting the volume with the highest diaphragm position. The planning CT was also obtained in exhale, using automated breathing control[19] or voluntary exhale breath hold (for patients treated with abdominal compression). The treatment isodose lines were converted into contours in 5-Gy increments between 0.5 and 55 Gy and perfusion parameters correlated to the corresponding dose level. Consequently, a linear regression was done of the changes in perfusion parameters K_{trans} and AUC at different time points throughout treatment. The strength of this correlation was compared with the received "normal" parenchyma dose.

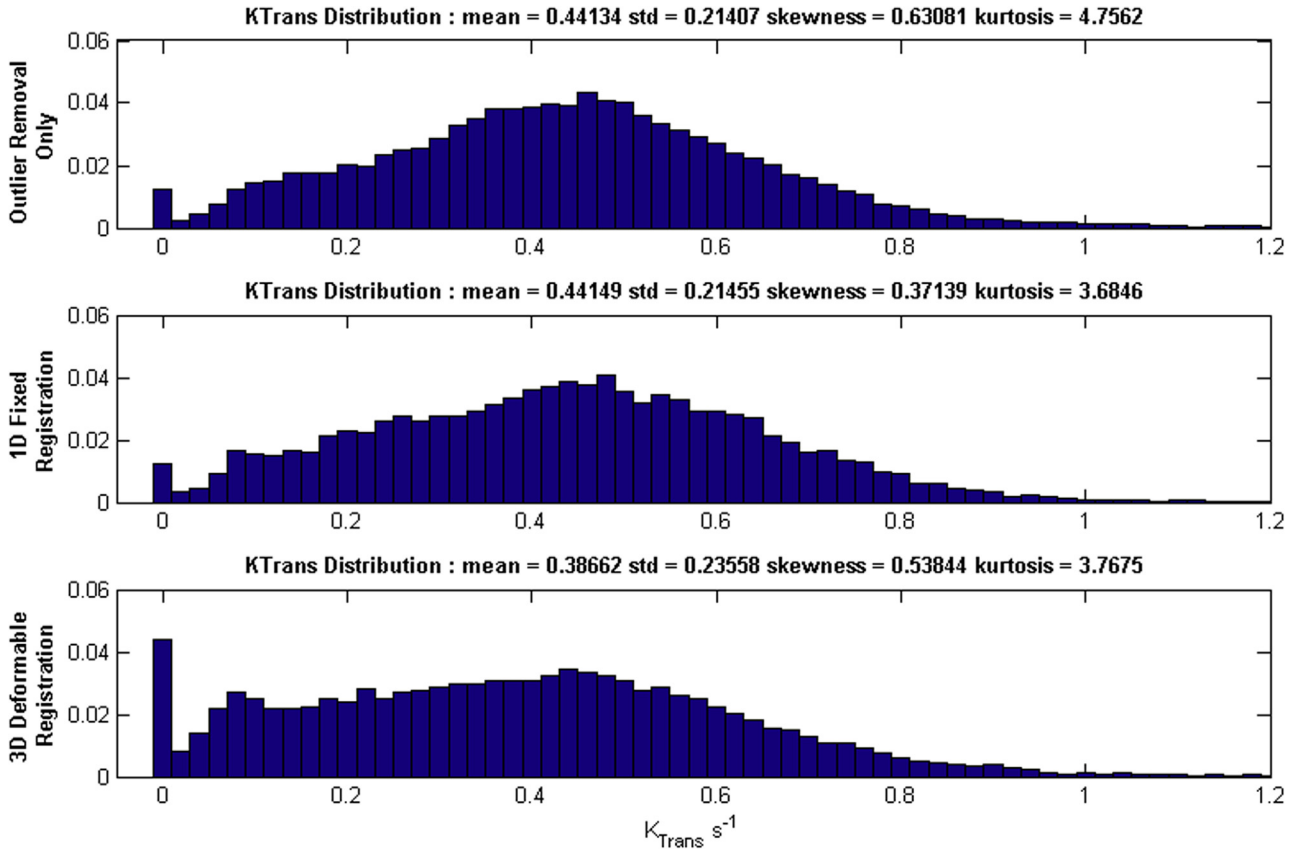

Figure 2 The effect of outlier removal, 1-dimensional rigid registration, and deformable registration on K_{trans} histograms. 1D, 1-dimensional; 3D, 3-dimensional; K_{trans}, kinetic parameters of perfusion.

Results

Image registration during DCE-CT acquisition

Deformable image registration was compared with the outlier method for the baseline scan of patient 1 and the resulting K_{trans} histogram of the tumor is displayed in Fig 2 for every method.

The 1-dimensional rigid and outlier removal methods both resulted in almost identical mean values and only slight variations in histogram shape. There was a subtle increase in the number of lower K_{trans} values for the deformable registration (as seen in the higher skewness and kurtosis values for the histogram), suggesting more of the necrotic region of the tumor was being included in the GTV for this patient. There will be limited uptake of contrast agent in the necrotic voxels because of low blood flow rates and higher interstitial fluid pressure,[20] resulting in a larger number of low K_{trans} values in the 3D histogram. For 3 of the 4 patients over the course of treatment ($n = 16$) the cutoff threshold consistently removed 8 of 69 data points (11.7%) with a standard deviation of 1.6 points (2.0%) for a coefficient of variation of 20.2%. The fourth patient was scanned with arms down, which greatly increased artifacts in the DCE-CT images; however, the algorithm still removed a consistent, if slightly higher, number of frames across all time points 15 of 69 (21.7%) with a standard deviation of 2 frames (2.8%), coefficient of variation 13.3%. In all cases, the method removed enough points to reduce the overall amount of motion while maintaining on average 87% of the frames to keep sufficient temporal information. Based on these results, it was determined that the outlier removal was effective at removing the more extreme breathing points, especially on the inhale phase, and that the rigid registration did not change the histograms in any meaningful way. From this point on, only outlier removal was applied within the analysis because it could be automated and is computationally inexpensive.

AIF: Individual sensitivity

Figure 3 shows the AIFs measured in the aorta at the level of the diaphragm at every time point for all patients. The difference in AIF peak shapes for patient 4 can be explained by the fact there was an unplanned pressure shutoff at intravenous injection during one of the pre-RT scan as well as at 1-month follow-up, hence partially contributing to the baseline variability. Contrast injection was not adjusted after the unplanned shutoff to allow for comparison between DCE scans. The unaffected baseline

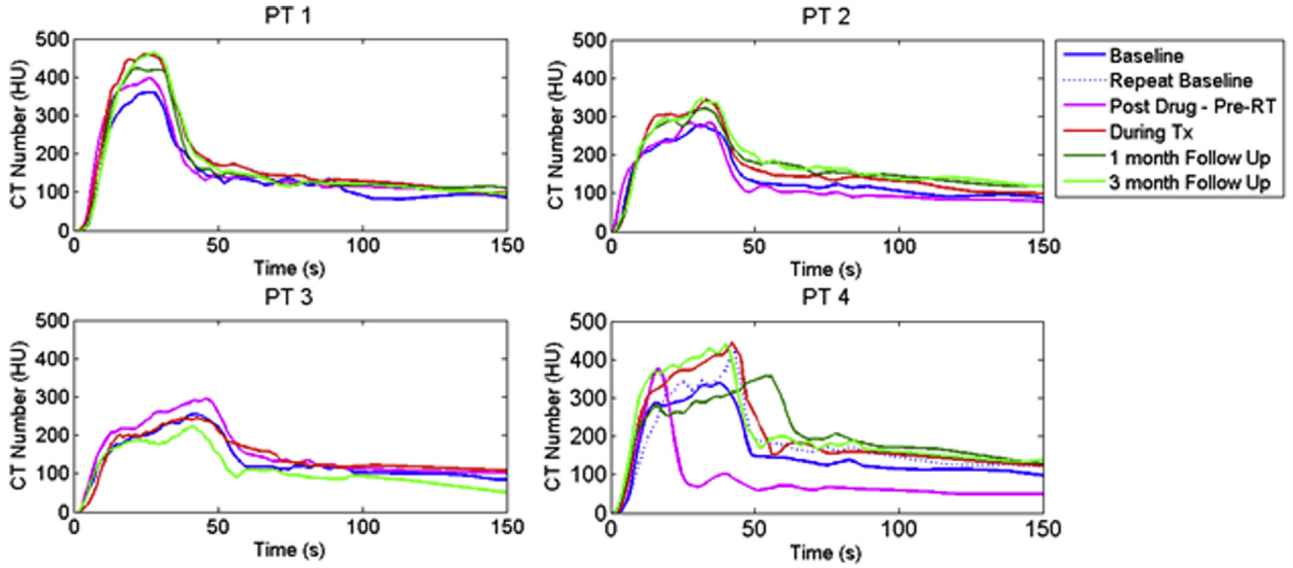

Figure 3 Arterial input function as measured in the aorta for different imaging days throughout treatment (Tx) for all 4 patients. CT, computed tomography; HU, Hounsfield units; PT, patient; RT, radiation therapy.

scan was used for further evaluation. There is a slight, gradual increase in the peak enhancement from baseline to progressively later imaging time points reaching a maximum difference of 20% for all patients except for the 3-month follow-up on patient 3, indicating a higher blood pressure as treatment continued (see Discussion), although the small number of cases did not allow for full significance ($P < .05$) to be reached. For the latter scan, the patient's arms were down, causing a lot of streaking artifacts in the DCE-CT scan.

Reproducibility of perfusion parameters

A repeat baseline DCE-CT scan was conducted in patient 4 and median perfusion values within each of the 3 GTVs as well as a control ROI in the liver parenchyma were compared as shown in Table 1. The percentage K_{trans} error ranged between 2% and 10% in the tumor ROIs (Pearson R = 0.93) and was 4% in the control ROI in unirradiated liver parenchyma (Pearson R = 0.86). Direct voxel-to-voxel correlation is more prone to errors in ROI registration; nevertheless, Bland-Altman analysis of K_{trans} values resulted in high coefficients of repeatability of (0.878, 0783, and 0.5) in tumor lesions A, B, and C, respectively, and 0.6 in the liver control ROI. The standard deviation in v_e and AUC was sometimes larger because they are more prone to the kinetic modeling fit and AIF shape.

Tumor vascular permeability and perfusion changes over time

Using the automated temporal dynamic analysis approach, it was possible to create 3D parameter maps and histograms describing the tumor vascular physiology and its heterogeneity. An illustration of changes in perfusion K_{trans}, permeability/interstitial space v_e, and AUC values over the course of treatment are shown in Fig 4 for patient 1 with HCC.

The pre-RT DCE-CT scan showed a decrease in tumor perfusion after administration of sorafenib compared with baseline as well as an increase in skewness and kurtosis of the perfusion histogram distribution in each tumor (Fig 5). Although statistically insignificant in this small group (K_{trans} − 14.8% ± 31.8%, $P > .5$), the trend was seen in all but 1 of the tumors that had a necrotic core.

During RT, tumor perfusion increased again and to levels higher than baseline perfusion in all but 1 case (patient 1, HCC) (K_{trans} + 16% ± 7.1%, $P = .013$), whereas permeability remained lower than baseline during RT for those same 5 tumors (v_e − 27.8 ± 15%, $P = .021$). Following RT, a significant decrease in perfusion was seen at 1 month relative to baseline in all but the same outlier (patient 1) (K_{trans} − 48.1% ± 37%, $P = .038$; v_e − 38.9 ± 37.0, $P = .087$). At 3 months following RT, K_{trans} had decreased even further (K_{trans} − 32.8 ± 23.2, $P = .0262$) but no permeability changes were noticeable.

Normal liver perfusion response to dose and sorafenib

The effects of radiation dose and sorafenib on normal liver parenchyma are illustrated in Fig 6 with an overall decrease in perfusion (Fig 6A) seen over the course of treatment for most cases. AUC measurements show little trending (Fig 6B). Measurements pre-RT, but after sorafenib administration, can detect some changes depending on the distance to the tumor (reduction in three-fourths of

Table 1 Variation in kinetic parameters as calculated from 2 baseline DCE-CT scans

Double baseline DCE-CT (patient 4)						
ROI	K_{trans} (L/min)	K_{trans} (% error)	v_e (L/min)	v_e (% error)	AUC (HU/s)	AUC (% error)
Tumor 4A	0.310 ± 0.032	10.23	0.26 ± 0.03	12.03	14,777 ± 1491	10.09
Tumor 4B	0.509 ± 0.012	2.45	0.26 ± 0.01	5.21	15,472 ± 2995	19.36
Tumor 4C	0.329 ± 0.020	6.09	0.22 ± 0.05	21.72	12,498 ± 465	3.72
Liver control	0.309 ± 0.013	4.12	0.22 ± 0.02	9.92	12,425 ± 1544	12.43
Mean		5.72		11.40		12.22

AUC, area under the curve; DCE-CT, dynamic contrast-enhance computed tomography; HU, Hounsfield units; K_{trans}, kinetic parameters of perfusion; v_e, extracellular volume.

patients). A strong dose-response is measured that is statistically significant ($P < .005$). The correlations between dose received and reduction in K_{trans} values at later time points are similarly statistically significant ($P < .05$) with correlation coefficients R^2 between dose and K_{trans} reduction beginning at −0.331 for pre-RT and becoming as strong as −0.95 at 3 months.

Discussion

In this initial exploratory study, it was investigated whether 4D DCE-CT of the liver was feasible under free breathing conditions and could detect spatial and temporal changes in both tumor and liver parenchyma perfusion and permeability in response to treatment. It was possible to generate voxel-based kinetic parameter maps in all patients using a temporal dynamic perfusion analysis method. In all but 1 case, a decrease in tumor perfusion was seen 1 week after administration of sorafenib but before RT, compared with baseline ($P = .035$, $n = 5$). This supports the hypothesis that sorafenib "normalized" the tumor vascularization, leading to decrease in interstitial tumor pressure and improving tumor perfusion. Coincidentally, the outlier corresponded to a case in which the intravenous injection suffered from a pressure shutoff. These results are in line with Cyran et al (2011),[21] who investigated the use of DCE-MRI for monitoring the effects of sorafenib on experimental prostate carcinoma with immunohistochemical validation. An interesting fact is that a higher peak AIF was measured postdrug/pre-RT by approximately 20%. Although this was not statistically

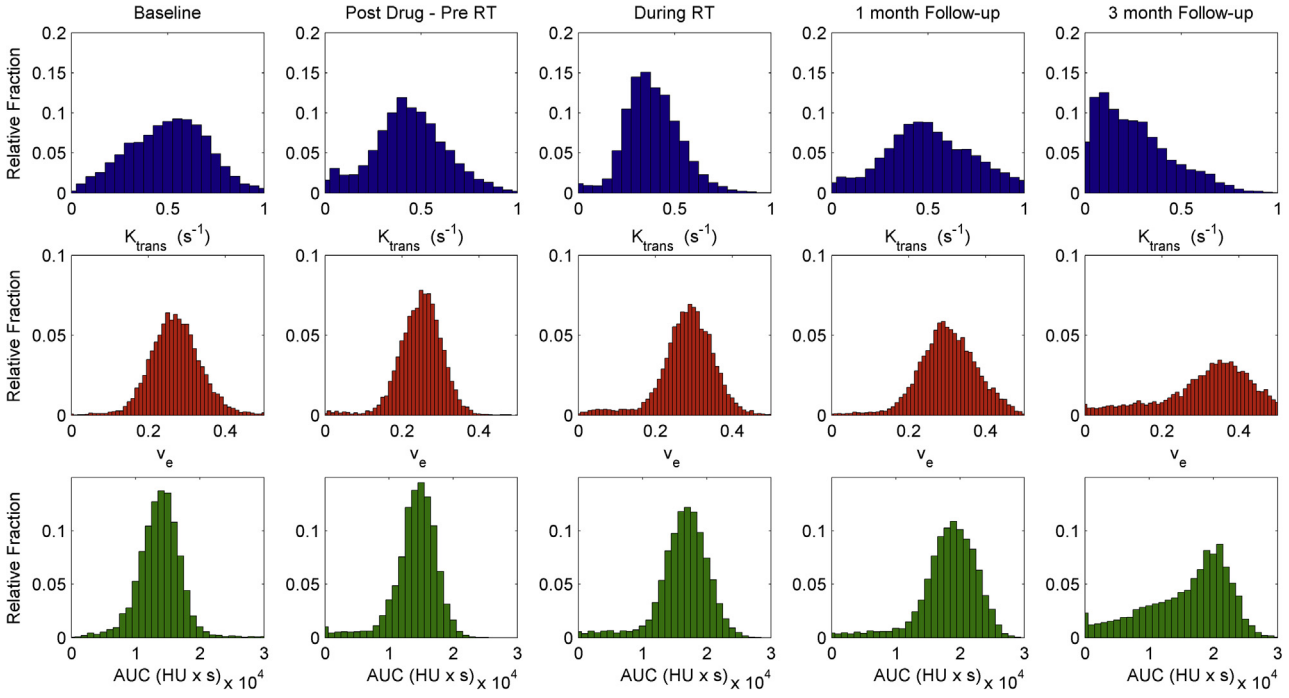

Figure 4 Kinetic modeling results for patient 1 over the course of treatment showing histograms of kinetic parameters in the tumor. (Top) Perfusion from the vasculature into the interstitial space (K_{trans}). (Middle) Permeability-fractional volume of the extravascular-extracellular space v_e. (Bottom) Median area under the curve (AUC) of signal enhancement. K_{trans}, kinetic parameters of perfusion; RT, radiation therapy.

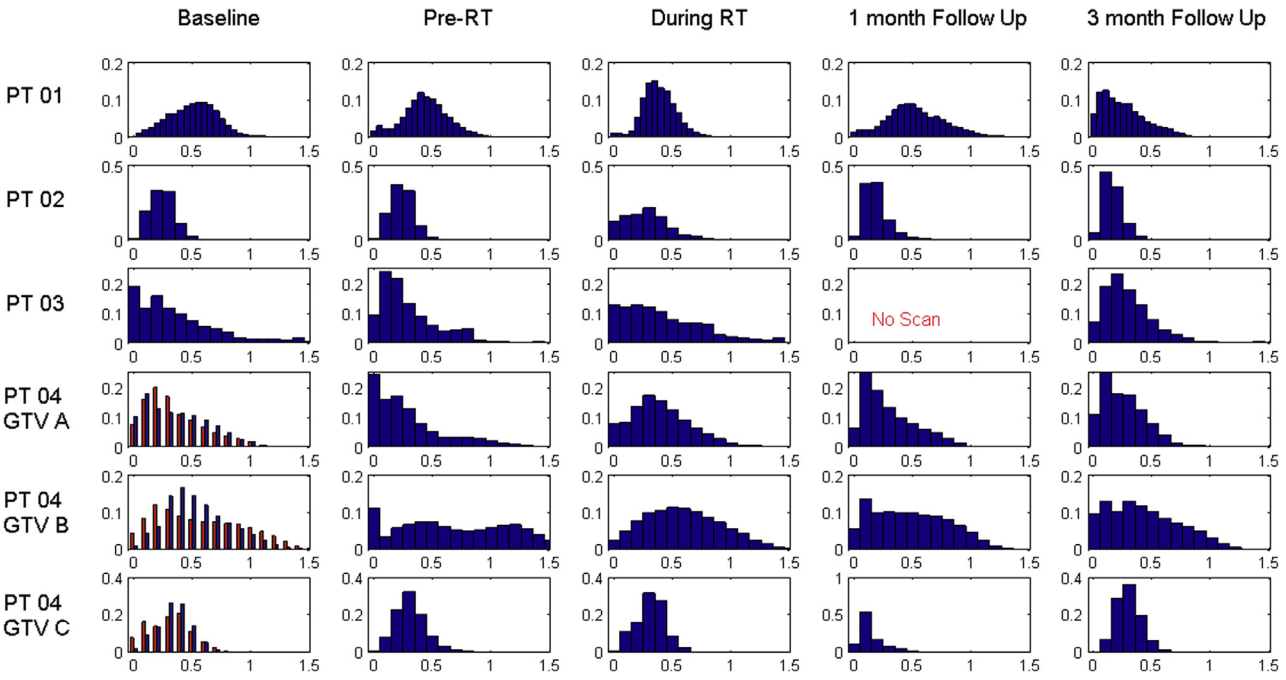

Figure 5 K_{trans} histograms for all 4 patients (6 tumors) over the course of treatment. The double baseline in patient 4 is overlaid in red. GTV, gross tumor volume; K_{trans}, kinetic parameters of perfusion; PT, patient; RT, radiation therapy.

significant in this small number of cases (n = 4), it could be hypothesized that this is correlated with sorafenib-induced hypertension as was previously reported.[22] Future studies with DCE-CT might replace a triphasic scan but only if the mAs at the respective arterial perfusion and parenchyma perfusion time points are increased above the low-dose DCE scanning settings and the full liver can be captured in the FOV.

During RT, tumor perfusion values increase again as can be understood from the fact that radiation damage results in cell apoptosis and an increase in extracellular space.[23] This is supported by an increase in interstitial

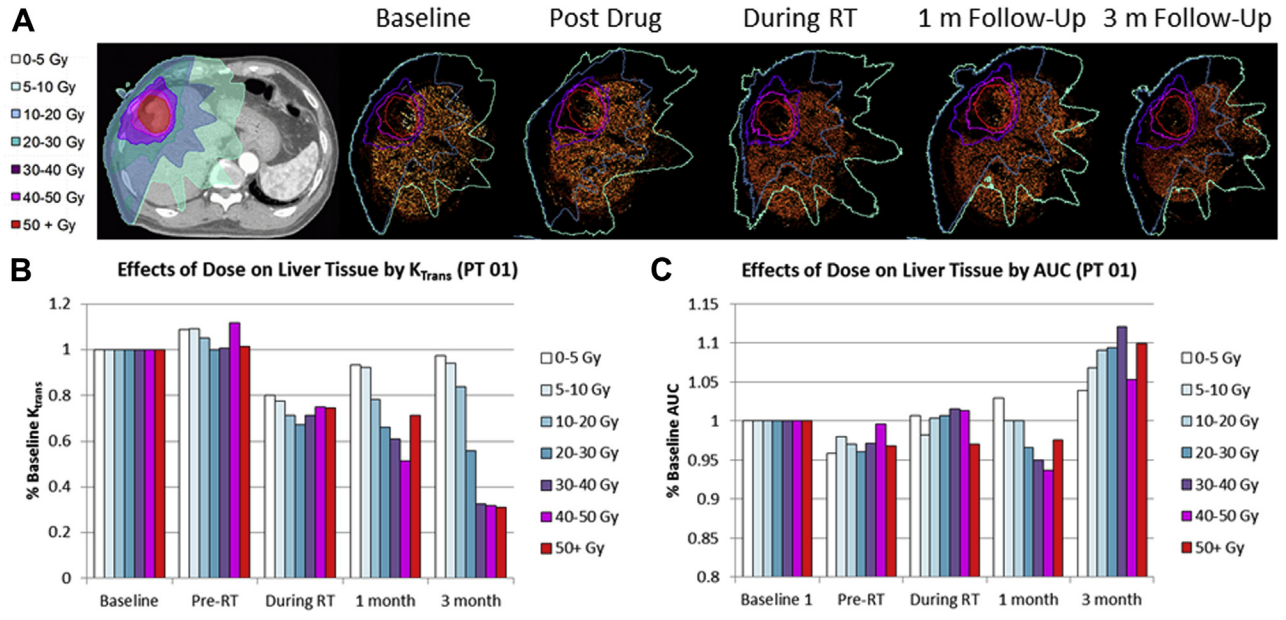

Figure 6 Effects of treatment on liver parenchyma perfusion (patient 1). (A) Illustration of dose distribution overlaid on CT image together with isodose lines over time. (B) Changes in median perfusion value K_{trans} over time and in function of received dose. (C) Changes in AUC from signal enhancement over time and in function of received dose. K_{trans}, kinetic parameters of perfusion; PT, patient; RT, radiation therapy.

volume, v_e. Following RT, tumor perfusion continues to decline for 5/6 cases. Histogram comparison over time for the outlier case suggests some level of renormalization at postdrug scan time with a high number of low-perfusion voxels that even out over the course of treatment, corresponding with the presence of the necrotic core. In these situations, it might be argued there is less need for biomarker analysis before standard Response Evaluation Criteria in Solid Tumors[24] change in tumors.

Double baseline DCE-CT scans indicated an average reproducibility of 5%, which is an order of magnitude better than perfusion variability reported previously using DCE scans 1 week apart on a 16-slice CT scanner,[25] as well as from DCE-MRI measurements.[26] This is likely also a conservative estimate given the unplanned pressure shutoff of 1 of the scans.

A limited number of publications has discussed perfusion CT for assessment of normal liver changes following radiation[27] and to the best of our knowledge no reports exist on the use of volumetric DCE-CT for tumor response evaluation and biomarker assessment for HCC and liver metastases. Figure 5 illustrates a strong dose-response effect on normal liver perfusion. Although the dose-response mechanism is compounded by the effect of sorafenib, the decrease in perfusion with increasing dose can be seen at 1 and 3 month following treatment by an approximate 1% reduction per Gy received ($R^2 = 0.9$, $P < .004$). This is similar to values reported by Cao et al (2008) using a 16-slice CT scanner and breath hold DCE-CT acquisition, who estimated a 1.2% reduction in venous perfusion per Gray. Careful definition of tumor volume and normal liver is clearly important as the voxels in the high-dose regions (50 Gy+) close to the tumor show an increase in perfusion that is likely from invisible tumor microscopic disease or underlying cirrhosis. Although not the focus of this work, describing the background liver as "normal" is something that needs to be verified in patients with liver malignancies, because many patients have underlying cirrhosis. In this study, all patients had Child-Pugh A scores and were treated on a prospective study with upfront DCE-CT and MRI. Platelet count was more than 70,000 and liver enzymes less than 6 times the upper limit of normal in all patients. No patients had active hepatitis or decompensated cirrhosis.

The AUC parameter of signal enhancement could not discriminate any changes in tumor perfusion, permeability, or dose-response effects and thus has little clinical utility. Although it is recognized that there were a small number of patients and tumors analyzed ($n = 6$), the lesions were found in all segments of the liver, with variable dose and size, providing a wide scope for feasibility testing.

The AIF functions in this study had relatively flat peaks which might be due to a slower injection protocol (4 mL/second) and/or volume of contrast being injected and less likely because of residual uncorrected respiration motion given the extent of intrascan image registration. It was shown in 1 case that the tumor histograms did not significantly change by using deformable image registration, and relative histogram changes over the course of treatment are much more pronounced than differences between double baseline and between motion correction strategies. Nevertheless, it is recognized that image registration between all phases of the DCE-CT scan could further improve the results but for this to be practically feasible 2 issues would have to be addressed. First, the advent of even larger scan FOV such as the 640-slice scanner could allow the entire liver to be present in all phases of the DCE-CT time sequence. This would have to be combined with improved liver autosegmentation capabilities, likely on a graphics processing unit cluster, to allow a deformable motion model to be created on the entire time sequence, which contains around 60 volumes in this case.

In summary, a volumetric perfusion CT methodology has been presented and demonstrated feasibility in obtaining 3D volumes of functional parameters such as perfusion and permeability of both tumor and parenchyma in patients with liver cancer. This is an important milestone toward achieving a voxel-based, quantitative functional imaging method that is sufficiently robust for use as a prognostic imaging biomarker in this challenging disease, thus setting the stage for larger validation studies.

Supplementary data

Supplementary material for this article (http://dx.doi.org/10.1016/j.adro.2016.06.004) can be found at www.practicalradonc.org.

References

1. Rudin M. Imaging readouts as biomarkers or surrogate parameters for the assessment of therapeutic interventions. *Eur Radiol*. 2007;17:2441-2457.
2. Kim SH, Kamaya A, Willmann JK. CT perfusion of the liver: principles and applications in oncology. *Radiology*. 2014;272:322-344.
3. Jain RK. Normalization of tumor vasculature: An emerging concept in antiangiogenic therapy. *Science*. 2005;307:58-62.
4. Coolens C, Driscoll B, Chung C, et al. Automated voxel-based analysis of volumetric dynamic contrast-enhanced CT data improves measurement of serial changes in tumor vascular biomarkers. *Int J Radiat Oncol Biol Phys*. 2015;91:48-57.
5. Driscoll B, Keller H, Jaffray D, Coolens C. Development of a dynamic quality assurance testing protocol for multisite clinical trial DCE-CT accreditation. *Med Phys*. 2013;40:081906.
6. Goh V, Ng QS, Miles K. Computed tomography perfusion imaging for therapeutic assessment: has it come of age as a biomarker in oncology? *Invest Radiol*. 2012;47:2-4.
7. Miles KA, Griffiths MR. Perfusion CT: A worthwhile enhancement? *Br J Radiol*. 2003;76:220-231.

8. Seppenwoolde Y, Shirato H, Kitamura K, et al. Precise and real-time measurement of 3D tumor motion in lung due to breathing and heartbeat, measured during radiotherapy. *Int J Radiat Oncol Biol Phys*. 2002;53:822-834.
9. Dawson LA, Ten Haken RK, Lawrence TS. Partial irradiation of the liver. *Semin Radiat Oncol*. 2001;11:240-246.
10. Coolens C, Breen S, Purdie TG, et al. Implementation and characterization of a 320-slice volumetric CT scanner for simulation in radiation oncology. *Med Phys*. 2009;36:5120-5127.
11. Brade AM, Kim J, Brierley J, et al. Phase I study of sorafenib and whole liver radiotherapy (WLRT) or stereotactic body radiotherapy (SBRT) for liver metastases. *Int J Radiat Oncol Biol Phys*. 2012;84:S11-S12.
12. Coolens C, Bracken J, Driscoll B, Hope A, Jaffray D. Dynamic volume vs respiratory correlated 4DCT for motion assessment in radiation therapy simulation. *Med Phys*. 2012;39:2669-2681.
13. Miles KA. Perfusion CT for the assessment of tumour vascularity: Which protocol? *Br J Radiol*. 2003;76:S36-S42.
14. Nguyen TN, Moseley JL, Dawson LA, Jaffray DA, Brock KK. Adapting liver motion models using a navigator channel technique. *Med Phys*. 2009;36:1061-1073.
15. Coolens C, Driscoll B, Chung C, et al. Automated voxel-based analysis of volumetric DCE-CT data improves the measurement of serial changes in tumor vascular biomarkers. *Int J Radiat Oncol Biol Phys*. 2015;91:48-57.
16. Driscoll B, Keller H, Coolens C. Development of a dynamic flow imaging phantom for dynamic contrast-enhanced CT. *Med Phys*. 2011;38:4866-4880.
17. Tofts PS, Brix G, Buckley DL, et al. Estimating kinetic parameters from dynamic contrast-enhanced T(1)-weighted MRI of a diffusable tracer: Standardized quantities and symbols. *J Magn Reson Imaging*. 1999;10:223-232.
18. Pandharipande PV, Krinsky GA, Rusinek H, Lee VS. Perfusion imaging of the liver: Current challenges and future goals. *Radiology*. 2005;234:661-673.
19. Eccles C, Brock KK, Bissonnette JP, Hawkins M, Dawson LA. Reproducibility of liver position using active breathing coordinator for liver cancer radiotherapy. *Int J Radiat Oncol Biol Phys*. 2006;64:751-759.
20. Hompland T, Ellingsen C, Galappathi K, Rofstad EK. DW-MRI in assessment of the hypoxic fraction, interstitial fluid pressure, and metastatic propensity of melanoma xenografts. *BMC Cancer*. 2014;14:92.
21. Cyran CC, Paprottka PM, Schwarz B, et al. Perfusion MRI for monitoring the effect of sorafenib on experimental prostate carcinoma: A validation study. *AJR Am J Roentgenol*. 2012;198:384-391.
22. Li Y, Li S, Zhu Y, et al. Incidence and risk of sorafenib-induced hypertension: A systematic review and meta-analysis. *J Clin Hypertension (Greenwich, Conn)*. 2014;16:177-185.
23. Kettunen MI, Brindle KM. Apoptosis detection using magnetic resonance imaging and spectroscopy. *Progr Nucl Magnet Res Spectrosc*. 2005;47:175-185.
24. Padhani AR, Ollivier L. The RECIST (Response Evaluation Criteria in Solid Tumors) criteria: Implications for diagnostic radiologists. *Br J Radiol*. 2001;74:983-986.
25. Ng CS, Chandler AG, Wei W, et al. Effect of dual vascular input functions on CT perfusion parameter values and reproducibility in liver tumors and normal liver. *J Comput Assist Tomogr*. 2012;36:388-393.
26. Wang H, Farjam R, Feng M, et al. Arterial perfusion imaging-defined subvolume of intrahepatic cancer. *Int J Radiat Oncol Biol Phys*. 2014;89:167-174.
27. Cao Y, Pan C, Balter JM, et al. Liver function after irradiation based on computed tomographic portal vein perfusion imaging. *Int J Radiat Oncol Biol Phys*. 2008;70:154-160.